Monolayer flow and in-plane orientation induced by a rotating disk in Langmuir and Langmuir-Blodgett films of a merocyanine dye

Keiichi Ikegami,[1,2] Christophe Mingotaud,[1] and Pierre Delhaés[1]

[1]*Centre de Recherche Paul Pascal, CNRS, Avenue A. Schweitzer, F-33600 Pessac, France*

[2]*Electrotechnical Laboratory, 1-1-4 Umezono, Tsukuba 305, Japan*

We have demonstrated that the rotating-disk method, which was proposed by Mingotaud *et al.* [J. Phys. Chem. **99**, 17 068 (1995)] recently, is effective to induce in-plane orientation in the Langmuir-Blodgett films of merocyanine dye–behenic acid mixtures. To clarify the orientation mechanism, the monolayer flow due to the disk has been observed directly and interpreted by an analytical model incorporating a non-Newtonian behavior of the films. Based on this observation, a steady-state orientation-distribution function has been calculated. The comparison of the calculated orientation-distribution function and the experimental data shows that our model gives a guideline of the rotating-disk method. [S1063-651X(97)12108-0]

I. INTRODUCTION

Organized molecular films have attracted much attention from scientific and technological points of view, because they provide a new platform for chemical and physical phenomena. A powerful tool to elaborate such new materials is the Langmuir-Blodgett (LB) technique [1]. Since this technique is based on the anisotropic adsorption of amphiphilic molecules onto the gas-liquid interface, it provides highly ordered structure along the normal axis of the substrate plane. On the contrary, the LB technique does not intrinsically induce the in-plane ordering, which is one of the most important properties of the ''well-organized'' films. Therefore, realizing in-plane organization of molecules or polymers in LB films is one of the most important issues in this research field [2].

Several researchers have reported in-plane anisotropy in LB films [3–10]. In most cases, the molecules are preferentially oriented parallel or perpendicular to the dipping direction of the substrate, indicating the important role of the monolayer transfer in the orientation mechanism. To explain this transfer-induced in-plane organization, ''flow-induced orientation models'' were proposed [11–13]. These models supposed that the origin of the observed anisotropy is the rotation of mesoscopic rodlike domains due to the monolayer flow [Figs. 1(a) and 1(b)]. Since this flow is generated by the monolayer transfer, they predict that larger dipping velocity gives rise to larger in-plane anisotropy until a saturation value. However, the possible range of the dipping velocity highly depends on the material, limiting the change in the dipping velocity as a method of obtaining higher in-plane organization [14].

Recently, a new method has been developed for controlling the in-plane orientation of Langmuir films by introducing a rotating disk at the gas-liquid interface [15]. The efficiency of this ''rotating-disk method'' has been demonstrated by using a substituted polyacrylate bearing side mesogenic group and a triazolehemiporphyrazine as film-forming materials. The orientation process has been qualitatively explained as follows. The rotating disk gener-

ates monolayer flow around it, characterized by a decrease in the rotation speed of the monolayer around the disk, $\omega(r)$, with increasing the distance from the center of the disk, r, i.e., $d\omega(r)/dr < 0$ when $\omega(r) > 0$. The velocity gradient causes shearing of the monolayer and mesoscopic rodlike domains should be preferentially oriented along the flow lines [Fig. 1(c)]. The generated in-plane orientation can be transferred onto solid substrates by adopting an appropriate dipping velocity [Fig. 1(d)]. Since the possible range of the shearing rate and that of the dipping velocity are determined by independent factors, we can choose the more effective method for a given Langmuir film. Furthermore, this rotating disk could be used to study hydrodynamical behavior of a monolayer as recently done by Friedenberg *et al.* with a ''four-roll mill'' system [16,17].
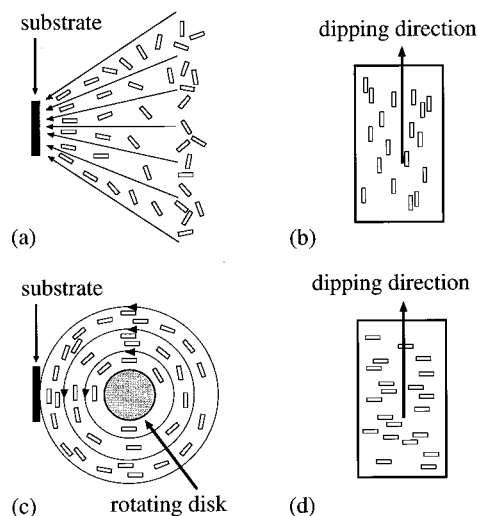

FIG. 1. Schematic illustrations of the in-plane orientation mechanism. (a) The flow orientation in the Langmuir film during the monolayer transfer. The motion of the substrate is perpendicular to the plane of this figure. (b) Molecular alignment within the plane of the built-up LB film as a result of the flow orientation. (c) The molecular orientation in the Langmuir film induced by a rotating disk. (d) Molecular alignment within the plane of the built-up LB film induced by a rotating disk.
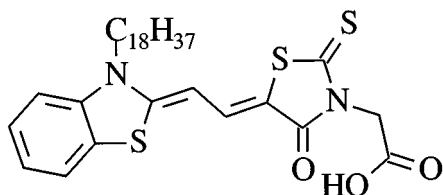
FIG. 2. Chemical structure of the merocyanine dye, DS.

With the rotating-disk method, the in-plane organization within a Langmuir film depends on the structure of the mesoscopic domains, the viscoelastic properties of the film, and the experimental setup (i.e., the size and the rotation speed of the disk, the relative position of the disk to the "observation point," and the shape and dimensions of the trough) [18,19]. To understand and control the effect of the rotating disk on the molecular orientation in the LB film, the influence of these three sets of parameters should be carefully estimated. One of the main points is to clearly relate the viscoelastic behavior of the monolayer with the efficiency of the rotating-disk method. Since the first consequence of a rotating disk is the shearing of the monolayer and the orientation of the domains is its second consequence, these two phenomena should be investigated separately. Therefore, we observed and semiquantitatively interpreted the velocity field (and the shearing) of mixed monolayers of a self-aggregating merocyanine dye DS (Fig. 2) with behenic acid (C_{22}). Then we calculated the steady-state orientation-distribution function of the mesoscopic rodlike domains in concentric flow and compared the calculated anisotropy with the experimentally obtained one. In addition, the observation of the velocity field of a monolayer having a large area may attract some interest from the rheological viewpoint.

In Sec. II we present the experimental methods. General characterizations of the Langmuir and LB films of the DS-C_{22} mixtures are given in Sec. III. In Sec. IV we describe the observation and analysis of the velocity field induced by a rotating disk. The optical dichroism in LB films induced by a rotating disk is discussed in Sec. V. Concluding remarks are given in Sec. VI.

II. EXPERIMENT

The merocyanine dye DS was purchased from The Japanese Research Institute for Photosensitizing Dyes, Co., and the behenic acid C_{22} from Fluka. Both compounds were used without further purification. Spreading solutions were prepared by mixing DS and C_{22} with a molar ratio of 1:x (x = 1, 2, or 4) and adding $CHCl_3$ as solvent and few drops of CH_3OH to the DS-C_{22} mixtures. The concentration of DS was ca. $1 \times 10^{-3} M$ (in the cases of $x = 1$ and 2) or ca. $5 \times 10^{-4} M$ ($x = 4$). The solution was spread on the pure-water subphase contained by an ATEMETA trough having dimensions of 38 cm×100 cm. The depth of the trough was about 11 cm in the part used for LB dipping and about 1 cm in the rest. A Millipore Milli-Q system was used for the purification of water and the resisitivity of the purified water was regulated to be larger than $1.8 \times 10^7 \ \Omega$ cm. Nitrogen gas was flowed into the housing of the trough with the rate of 1700 liters an hour to minimize the dissolution of carbon dioxide and oxygen into the subphase. Surface-pressure isotherms

were obtained by using a step-by-step compression method.

A rotating disk made of Teflon was introduced at the gas-liquid interface [15]. The diameter and the height of the disk were 5 and 1 cm, respectively. For the observation of the monolayer flow the disk was mechanically set at the center of each monolayer having dimensions of ca. 38×38 cm^2. For the fabrication of LB films, the distance between the substrate and the center of the disk was varied. The disk rotates with a constant rotation speed before spreading the solution. The rotation speed of the disk, ω_{disk}, was set to 0.63, 2.1, or 6.3 rad/s for the observation of the flow and to 2.1 or 6.3 rad/s for the fabrication of LB films.

The observation of the monolayer flow and the LB deposition were performed at a surface pressure of 15 and 25 mN/m and of 25 mN/m, respectively. Here, the compression of the monolayer was done within 25 min and the compressed monolayer was used within 60 min to obtain a reasonable formation of J aggregates. Plates of CaF$_2$ ($3 \times 1 \times 0.2$ cm^3) were used as substrates after being precoated with three layers of C_{22}. Twenty layers of the DS-C_{22} mixtures were transferred by the conventional vertical dipping method. The deposition was Y type with a transfer ratio close to unity. The distance between the substrate and the edge of the trough was 2.4 cm.

To measure the flow velocity of the monolayer, grids for the transmission electron microscope (Aldrich, made of nickel) were put on the monolayer as floats and their trajectories were observed by a Hamamatsu charge-coupled device (CCD) camera. The images were digitized and analyzed by using a microcomputer and NIH image software [20]. The velocity of a small part of the monolayers (dr/dt and $\omega \equiv d\psi/dt$ in the cylindrical coordinate system whose origin is fixed at the center of the disk), which is represented by the velocity of a float on it, was measured by using three sequential "snap shots" taken by the CCD camera. The acceleration (d^2r/dt^2 and $d\omega/dt$) was also determined.

Perkin-Elmer 330 and Nicolet Magna-IR 750 spectrometers were used for the visible and IR polarized absorption spectroscopy. The orientation of the transition dipole moment μ of the molecules within the LB films was determined by linear dichroism using IR spectroscopy [21,22]. We measured three different polarized IR spectra varying the direction of E, where E is the local IR electric field. In the first two cases, E is in the film plane (the incident angle, i.e., the angle between the substrate normal and the IR beam, is 0°) and either parallel or perpendicular to the dipping direction of the substrate. We obtain then the absorption of the IR band associated to μ, $A_\parallel(0°)$, and $A_\perp(0°)$, respectively. In the third case, the incident angle is 60° and E is in the plane determined by the incident beam and the substrate normal. We denote the absorption mesured in this case as $A_\parallel(60°)$, since with our experimental setup the projection of E onto the film plane is parallel to the dipping direction. Based on the Snell-Descartes relation, Chollet and Messier developed a theory giving the refraction angle (and then the direction of E) as a function of the incident angle and the refractive indices of the three media, i.e., the atmosphere, the LB film, and the substrate [22]. By using this theory we can deduce the direction of μ from these three absorption values, since $A \propto (\mu \cdot E)^2$.
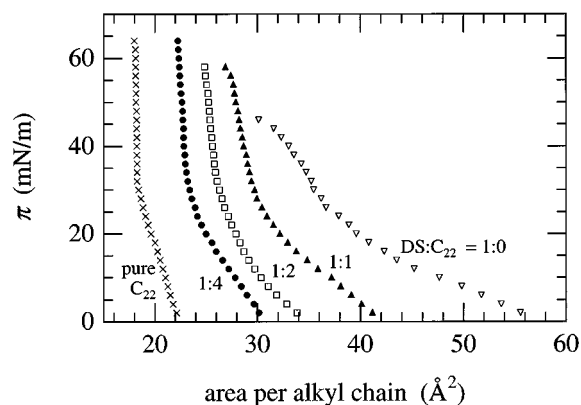
FIG. 3. Surface pressure (π)-area isotherms of the Langmuir films of the DS-C_{22} mixtures. The mixing molar ratios are 1:0 ($\triangledown$), 1:1 ($\blacktriangle$), 1:2 ($\square$), and 1:4 ($\bullet$). The isotherm of the pure C_{22} film is also indicated ($\times$).

FIG. 4. Visible absorption spectra observed for an LB film (20 layers on each side of the substrate) of the 1:1 mixture of DS and C_{22} with the electric vector of the incident light being parallel (solid line) and perpendicular (broken line) to the dipping direction of the substrate, respectively, and those for an LB film of pure DS (thin and dotted lines, respectively). (These films were fabricated without a rotating disk.)

III. GENERAL CHARACTERIZATION OF THE MATERIAL

We have avoided including metallic ions in the Langmuir and LB films of the DS-C_{22} mixtures to minimize the monolayer-subphase ionic interaction as well as the chemical complexity of the system. Some general characterizations of the present system were needed before investigating the effect of the rotating disk, since the DS-C_{22} films on the pure-water subphase have not been intensively studied, while there are many reports on those on the metal-ion containing subphase [3–5,23–29]. Moreover, the obtained results provide information about the formation of the J aggregates of DS, which is also an interesting subject in this research field, although it is not the main purpose of this paper.

A. Monolayers at the gas-liquid interface

Figure 3 shows the π-A isotherms of DS-C_{22} 1:x mixtures, with $x = 0$, 1, 2, and 4. The isotherm of pure C_{22} is also indicated. The curves exhibit more compressed behavior than that observed on the Cd-containing subphase [5,23], suggesting different molecular arrangement with respect to the normal axis of the gas-liquid interface.

The collapse pressure depends on the mixing ratio. The mixing-ratio dependence of the occupied area per alkyl chain (defined as A_{chain}) deviates from the ideal mixing behavior [30]. Between $x = 1$ and 4 a linear variation is observed; i.e., A_{chain} is well reproduced by $A_{chain} = 23/(1+x) + 19x/(1+x)$ $Å^2$ at 25 mN/m. The areas occupied by one DS molecule and one C_{22} molecule could then be estimated at 23 and 19 $Å^2$, respectively, in these mixtures. The latter value coincides with the isotherm of pure C_{22}. On the contrary, the area occupied by DS in the pure film ($x = 0$) is 37 $Å^2$ at 25 mN/m. These facts deny macroscopic phase separation of DS and C_{22} at least in the 1:1 film.

The estimated three basic cross-sectional areas of the DS molecule are 122 $Å^2$ in the chromophore plane, 57 $Å^2$ normal to the short axis, and 28 $Å^2$ normal to the long axis, respectively [5]. In comparison with these values, the above obtained occupied area of DS in the mixed films seems to be too small. This may suggest the interdigitation of the C_{22}
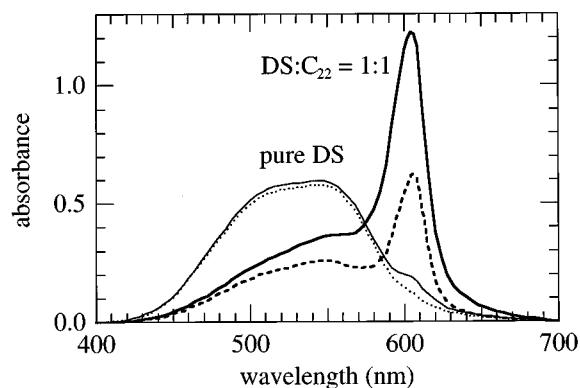
molecules between the alkyl chains of the DS molecules forming J aggregates [31].

The initial color of the monolayers is pink, but it gradually changes to blue in the mixed cases, implying the formation of the J aggregates at the gas-liquid interface. This change in color, which was observed directly on the trough, seems to be affected by the surface pressure: intermediate pressure (2–10 mN/m) may promote the aggregation of the DS dye.

B. Optical properties of the LB films

A prominent J band is observed around 603 nm in the visible absorption spectra of the LB films of the 1:1, 1:2, and 1:4 mixtures of DS and C_{22}, while we detect only a trace of this band in the pure film (Fig. 4). Other authors assigned the bands around 550 and 510 nm to the monomeric and dimeric absorption, respectively [23]. The peak position and the spectral shape of the J band are found to be almost identical for the 1:1, 1:2, and 1:4 mixtures, suggesting a similar structure of the J aggregates in the LB films of those mixtures. Furthermore, the peak position of the J band observed for the present system is compatible with those observed for the Langmuir films of the DS dye formed on the subphase containing divalent ions or LB films made from them [3,24,25,28].

Figure 5 shows the IR spectra observed for LB films of pure DS, DS-C_{22} 1:1 mixture and pure C_{22}. The preliminary assignment of the IR bands was carried out on the basis of Fujimoto et al.'s work [25,26]. Although the absorption from the precoated films (each consisting of 3 layers of C_{22}) causes a small error in the quantitative characterization, we can extract information concerning the arrangements of the alkyl chains in the present system. The peak positions (2921 and 2852 cm^{-1}) and the linewidth of the antisymmetric and symmetric stretching bands of the CH_2 group [$\nu_a(CH_2)$ and $\nu_s(CH_2)$] observed for the pure DS films show that a large portion of the C-C bonds in the alkyl chain should have a gauche conformation. On the contrary, these bands in the mixed films are located at lower wave numbers (2916 and
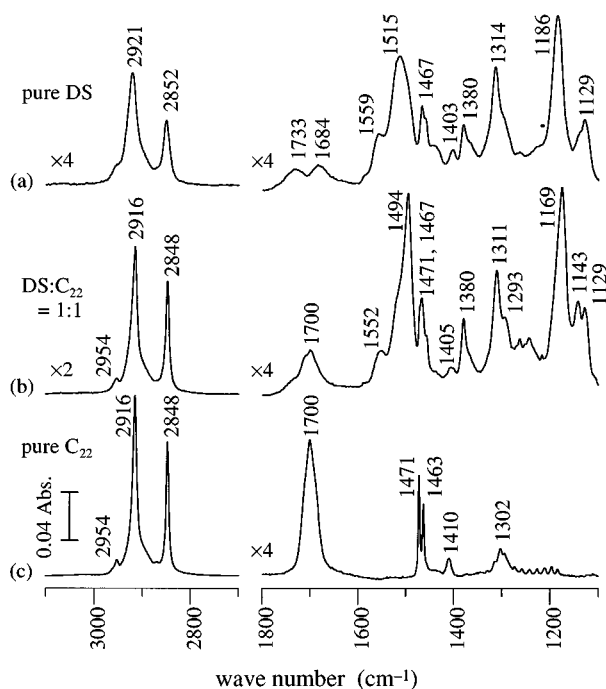
FIG. 5. FT-IR absorption spectra for LB films (20 layers on each side of the substrate) of (a) pure DS, (b) DS-C_{22} 1:1 mixture and (c) pure C_{22}. The electric vector of the incident light is parallel to the dipping direction of the substrate.
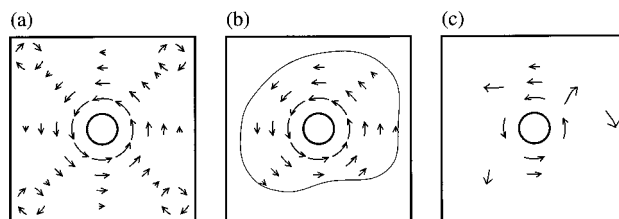

FIG. 6. Schematic illustration of the flows induced by a rotating disk. (a) A regular flow recorded for the 1:2 and 1:4 mixtures of DS and C_{22}. (b) an irregular flow observed for the 1:1 mixture. In this case a clear boundary dividing the monolayer into two regions, which is illustrated by a thin line, can be seen and the flow is observed only in the inner region. (c) Example of a completely irregular flow recorded for the pure water surface.

2848 cm^{-1}) with narrower linewidth, reflecting the dominance of the trans conformation in the C-C bonds as in the case of the pure C_{22} films. The polarization spectroscopy has led to an estimation of the averaged angles (see Sec. II) between the dipole moments of $\nu_a(CH_2)$ and $\nu_s(CH_2)$ modes and the normal axis of the substrate: ca. 66° and 71°, respectively, for LB films of 1:1 mixture of DS and C_{22}. In other words, the averaged angle between the alkyl chain axis and the normal axis of the substrate is about 32° in 1:1 mixed films. This tilt angle decreases when the mole fraction of C_{22} is increased, and it reaches a value ca. 12° for LB films of the 1:4 mixture of DS and C_{22}.

The shifts of the bands of the carboxylic group (1700–1800 cm^{-1}) may suggest intramolecular or intermolecular hydrogen bonds for DS molecules, respectively, in the pure or mixed films. The former result is compatible to that reported for pure DS solid (powder) [26]. The IR spectra in the 1600–1100 cm^{-1} region of the mixed LB films are similar to those reported for the LB films of pure DS with Ba^{2+} ions [25]. No significant difference in this region was detected among the LB films of the DS-C_{22} 1:1, 1:2, and 1:4 mixtures, except for the intensity ratio of the bands due to the DS and C_{22} moieties. The bands seen in the regions of 1560–1490 and 1190–1140 cm^{-1} may be attributed to the central conjugated system of the DS molecule, since they show significant change in their positions and/or intensities when the J band appears in the visible spectrum. The formation of the J aggregates may modify the electronic distribution and then change the bond strength and the dipole strength [27]. The polarization spectroscopy has shown that the angles between the normal axis of the substrate and the dipole moments corresponding to the peaks around 1494, 1169, and 1143 cm^{-1} in the mixed LB films are larger than

75°, where those corresponding to 1515, 1186, and 1129 cm^{-1} in the pure DS films are about 60°.

From the observed π-A isotherms and optical characteristics, we conclude that the J aggregates of the DS molecules are formed on the pure-water subphase and can be transferred onto solid substrates. The important role of C_{22} in the formation of the J aggregates in the 1:1 mixture is implied. The influence of the excessive C_{22} on the structure of the aggregates is negligible. However, the viscoelastic properties of the monolayer depend highly on the mixing ratio, as demonstrated by the measurement of the monolayer velocity field under shearing.

IV. MONOLAYER FLOW INDUCED BY A ROTATING DISK

In order to quantitatively understand the orientation mechanism of the rotating-disk method, observation and modeling of the monolayer flow induced by the disk are essential. The experimental results and the phenomenological models described in this and the next section elucidate the important factors of the rotating-disk method, providing a guideline for a better application of it.

A. Observation of the velocity field

The monolayer flow induced by a rotating disk having a radius (r_{disk}) of 2.5 cm was observed for the 1:x ($x = 1$, 2, and 4) DS-C_{22} mixtures as well as pure C_{22}. In the case of $x = 2$ and 4 as well as the pure C_{22} case the observed monolayer flow was regular and approximately concentric, although vortices were detected at the corners of the monolayers [Fig. 6(a)] [32]. For the 1:1 mixture approximately concentric flow was observed at 15 mN/m, but at 25 mN/m sometimes a macroscopically inhomogeneous structure of the monolayer was observed [Fig. 6(b)]. It should be mentioned that the observed flow of the pure water surface was irregular and not stationary [Fig. 6(c)], probably due to complex three-dimensional flow.

In fact, dr/dt, d^2r/dt^2, and $d\omega/dt$ measured for the 1:2 and 1:4 mixtures were practically zero, confirming that the monolayer flow of these mixtures is approximately concentric. Typical data of the r dependence of ω measured under the above conditions are shown in Figs. 7(a) and 7(b) for $x = 2$ and 4 mixtures, respectively. The striking features of the observed velocity field are the nonlinearity of $\omega(r)$ with re-
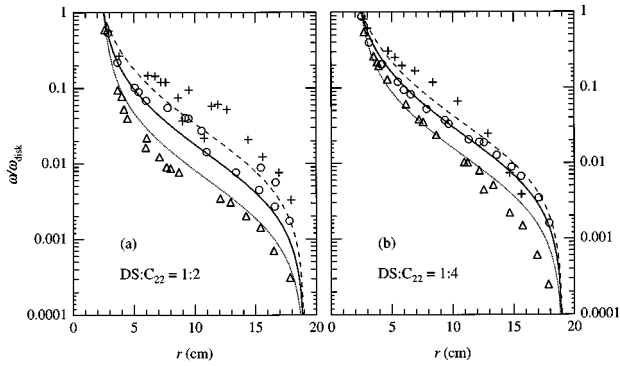
FIG. 7. Typical r dependence of the normalized angular velocity, $\omega/\omega_{\text{disk}}$, of the 1:2 (a) and 1:4 (b) mixed monolayers of DS and C_{22}. The rotation speed of the disk, ω_{disk}, is 6.3 ($\triangle$), 2.1 ($\bigcirc$), or 0.63 rad/s (+). Simulated curves calculated by using Eq. (3) with $K=0.4$ and 1.0 s^{-1} for the 1:2 and 1:4 mixtures, respectively, are also indicated. These curves correspond to ω_{disk} of 6.3 (dotted lines), 2.1 (solid lines), and 0.63 rad/s (broken lines). It should be noted that the simulated curves for $\omega_{\text{disk}}=0.63$ rad/s are not so much deviated from the one calculated with Eq. (1).

spect to ω_{disk} and the steep decrease of $\omega(r)$ in the small-r region. On the other hand, the observed finite velocity in the large-r region is quite natural if the plasticity of the monolayer is small. It should be noted that similar results are obtained for pure C_{22} monolayers.

Because the in-plane orientation is related to the shearing rate G as discussed in Sec. V, the evaluation of G should be made in order to estimate the effect of the rotating disk. This value is given by twice the off-diagonal component of the deformation speed tensor, which is the symetrical part of the velocity gradient tensor [33]. In a concentric flow, therefore, we obtain $G=rd\omega(r)/dr$ [33,34]. The experimental data of G obtained for the Langmuir films of the 1:2 and 1:4 DS-C_{22} mixtures are indicated in Figs. 8(a) and 8(b), respectively. The shearing rate for $r>4$ cm with given ω_{disk} is higher in the case of the 1:4 mixture when compared to the 1:2 system. Such behavior demonstrates that the effect of the
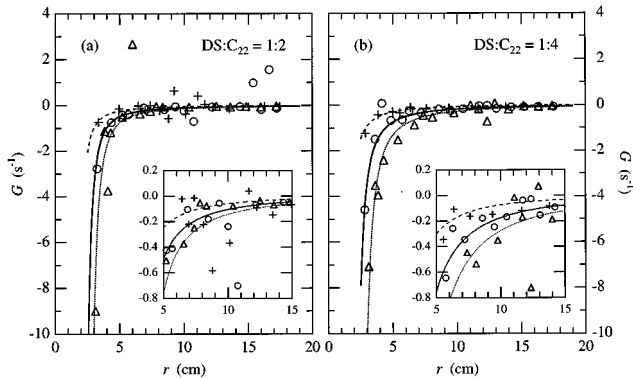

FIG. 8. Typical r dependence of the shearing rate, $G = rd\omega(r)/dr$, of the 1:2 (a) and 1:4 (b) mixed monolayers of DS and C_{22}. The rotation speed of the disk, ω_{disk}, is 6.3 ($\triangle$), 2.1 ($\bigcirc$), or 0.63 rad/s (+). Simulated curves calculated by using Eq. (3) with $K=0.4$ and 1.0 s^{-1} for the 1:2 and 1:4 mixtures, respectively, are also indicated. These curves are corresponds to ω_{disk} of 6.3 (dotted lines), 2.1 (solid lines), and 0.63 rad/s (broken lines). The insets are respective expansions of the region of $5<r<15$ cm.

rotating disk highly depends on the type of Langmuir film used for the experiment.

B. Model of the flow

Since the in-plane orientation in the LB film depends on the shearing induced by the rotating disk, the origin of the decrease of $\omega(r)$ with the distance should be clarified. Three basic factors can govern this decrease: (i) a Newtonian behavior of the Langmuir film, (ii) interactions between the film and the subphase, and (iii) non-Newtonian properties of the film. To evaluate the effects of these factors, the experimentally observed monolayer flow at the gas-liquid interface was theoretically fitted to the simple and realistic models that we could suggest.

Approximating that the trough has a rounded shape with a radius of $r_{\text{trough}}=19$ cm [35], we can apply the well-known simple torque equation [33,34]: in the stationary state, the torque applied to the ring part $[r,r+dr]$ of the monolayer from the inner and outer parts, $M(r)$ and $-M(r+dr)$, respectively, should be identical, because this ring is not accelerated. The torque is given by the product of the distance r, the circumference $2\pi r$, and the shearing stress σ. If we assume that the monolayer behaves as a Newtonian fluid with a surface viscosity of η_L, we readily obtain

$$\omega(r) = \frac{M}{4\pi\eta_L}\, r^{-2} + C_1 \quad (\text{for } r\neq 0), \qquad (1)$$

Here, the constant torque M and the constant C_1 are determined by the boundary conditions of $\omega(r_{\text{disk}})=\omega_{\text{disk}}$ and $\omega(r_{\text{trough}})=0$. However, experimentally obtained $\omega(r)$ decreases more rapidly with increasing r than Eq. (1) when ω_{disk} is large, although this equation well fits the data for $\omega_{\text{disk}}=0.63$ rad/s.

One possible origin of this rapid decrease could be a dissipative interaction between the monolayer and the subphase [36]. However, this interaction may not induce the observed nonlinearity and not fit the obtained r dependence of $\omega(r)$ for any given ω_{disk} (see Appendix).

Non-Newtonian behaviors, i.e., yield value, dilatant, and pseudoplastic behaviors, of the monolayers could be other possible origins of the rapid decrease of $\omega(r)$. If the shearing rate realized under the experimental conditions is ''small,'' the lowest-order correction terms could reproduce the non-Newtonian behaviors. Along this line, we performed preliminary calculations (see Appendix). Such models suggested that the pseudoplastic behavior could cause the rapid decrease of $\omega(r)$ and induce the observed nonlinearity, but they also showed that the lowest-order approximation used to describe such pseudoplastic monolayer breaks because the shearing rate realized under these experimental conditions is *not* ''small.''

Therefore, we approximate the pseudoplastic property not only by a lowest-order correction, but by a hyperbolic sine function, which was theoretically introduced by Eyring for a three-dimensional system [37,38]. His calculation is based on a one-dimensional rate process with a potential energy barrier; the difference between the forward and backward hopping rates of a molecule, which are originally identical and changed by the presence of shearing, leads to

$$\sigma = \eta K \sinh^{-1}(G/K). \qquad (2)$$

Here, η and K are the ''viscosity'' of the three-dimensional system in the linear region and the crossover shearing rate between the linear and the nonlinear region, respectively [39]. Since his theory is based on a one-dimensional hopping along the velocity field, such an equation can be applied also to Langmuir films (with a surface viscosity of η_L instead of η) [40]. Then, we readily obtain

$$\omega(r) = \omega_{\mathrm{disk}} - \int_{r_{\mathrm{disk}}}^{r} K\rho^{-1} \sinh\left(\frac{M}{2\pi \eta_L K} \rho^{-2} \right) d\rho, \quad (3)$$

where the value of the torque M should be determined by the boundary condition of $\omega(r_{\mathrm{trough}}) = 0$.

Equation (3) reproduces the data satisfactorily with $K = 0.4$ and $1.0\ \mathrm{s}^{-1}$ for the 1:2 and 1:4 mixtures of DS and C_{22}, respectively, as shown by the curves in Figs. 7(a) and 7(b). The calculated shearing rate also acceptably fits the experimental data (Fig. 8). Note that we have only one fitting parameter, K [41], and we must use the same K value with different ω_{disk} values to describe one kind of monolayer. The difference in K reflects the difference in the viscoelastic properties of these mixtures: the pseudoplasticity is more remarkable in the 1:2 mixture than in the 1:4. It might be correlated to the change in alkyl chain density and then to the lateral interactions within the Langmuir film. Knowing that the pseudoplasicity of the monolayer is the main factor controlling the shearing, we then analyzed the in-plane orientation in LB films.

V. IN-PLANE ORGANIZATION OF LB FILMS

In this section we intend to demonstrate the efficiency of the rotating-disk method on Langmuir films of the DS-C_{22} mixtures and model the orientation mechanism under the shearing field, which can be calculated based on the monolayer hydrodynamical behavior presented in Sec. IV. Before discussing the effect of a rotating disk, however, we need to characterize the in-plane orientation of the DS-C_{22} mixed LB films deposited without a rotating disk.

A. In-plane orientation without a rotating disk

A clear correlation was observed between the appearance of the J band and the in-plane dichroism in both the visible and IR spectra. Indeed, the IR peaks around 1494, 1169, and 1143 cm^{-1} in the mixed LB films (assigned to the central conjugated system of DS) exhibit dichroic behavior compatible with that of the J band. This is established by comparing the visible and IR dichroisms of a LB sample, indicated in Fig. 4 (solid and broken lines) and Fig. 9 (thick and thin lines), respectively. This agreement is maintained in the LB films prepared by using the rotating-disk method. In the following, we choose the IR absorption band around 1143 cm^{-1} to characterize the in-plane anisotropy of the mixed LB films, because this band is associated to the J aggregate and well separated from monomeric bands.

The in-plane order parameter P_2 of the LB films is defined as $P_2 \equiv \langle \cos(2\theta) \rangle$, where θ is the angle between the projection of the transition dipole moment onto the film plane and the dipping direction of the substrate and $\langle \ \rangle$ de-
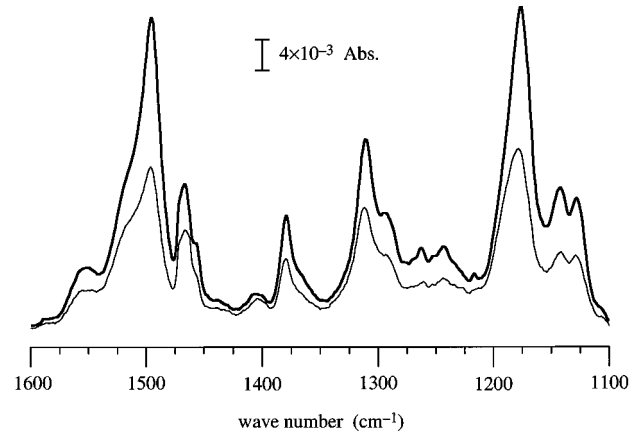

FIG. 9. Dichroism observed in the FT-IR spectrum of the LB film of the DS-C_{22} 1:1 mixture whose visible dichroism is shown in Fig. 4. (This film was fabricated without a rotating disk.) Thick and thin lines represent the spectra with the electric vector of the incident light being parallel and perpendicular to the dipping direction of the substrate, respectively.

notes the average over the molecular distribution within the LB film. Note that this definition of P_2 is applicable to the LB films fabricated with the rotating-disk method, if they are Y type so that the mirror symmetry with respect to the dipping direction can be assumed [19]. This P_2 parameter can be determined by the observed in-plane optical dichroism of the absorption band associated with the transition dipole moment under consideration as

$$P_2 = \frac{A_{\parallel}(0°) - A_{\perp}(0°)}{A_{\parallel}(0°) + A_{\perp}(0°)}. \qquad (4)$$

Here, $A_{\parallel}(0°)$ and $A_{\perp}(0°)$ are the optical absorbance of the film with the polarization of the incident light being parallel and perpendicular to the dipping direction of the substrate, respectively (see Sec. II). When a LB film has a domain structure, P_2 is given by the product of two ''partial'' in-plane order parameters:

$$P_2 = P_2^{\mathrm{moment|domain}} P_2^{\mathrm{domain|substrate}}, \qquad (5)$$

where $P_2^{\mathrm{moment|domain}}$ is the order parameter of the dipole moments with respect to the long axes of the domains and $P_2^{\mathrm{domain|substrate}}$ is that of the long axes of the domains with respect to the dipping direction of the substrate.

The in-plane anisotropy observed for the LB films fabricated with a normal dipping method (without rotating disk) can be explained by the ''flow-induced orientation model'' [11–13]: the rodlike mesoscopic domains are preferentially oriented along the dipping direction. In this case $P_2^{\mathrm{moment|domain}}$ is determined by the structure of these rodlike domains, while $P_2^{\mathrm{domain|substrate}}$ is determined by the flow orientation.

B. In-plane orientation induced by a rotating disk

We have demonstrated that the rotating-disk method is effective also for the DS-C_{22} mixed films, although the real efficiency depends on the mixing ratio. In Fig. 10 the P_2 data
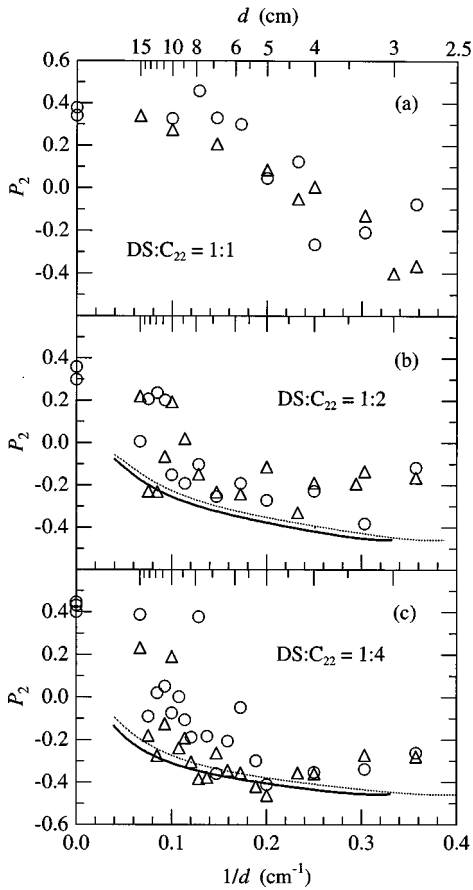
FIG. 10. The P_2 data observed for LB films of DS-C$_{22}$ 1:x mixtures transferred by the rotating-disk method are plotted against the inverse of the distance between the dipping position and the center of the rotating disk, d^{-1}. The mixing ratios are (a) $x=1$, (b) $x=2$, and (c) $x=4$. The rotation speed of the disk, ω_{disk}, is 6.3 ($\triangle$) or 2.1 rad/s ($\bigcirc$). The dipping velocity is 0.028 cm/s. Here we take d^{-1} for the abscissa to expand the region near the disk and to include the P_2 data obtained without disk, which is plotted at $d^{-1}=0$. For the 1:2 and 1:4 mixtures simulated curves calculated by using Eq. (9) with the parameters of $P_2^{\mathrm{moment|domain}}=0.55$, $\zeta=7\times10^{-12}$ erg s and $\tau_0=6\times10^{-14}$ erg are also indicated. (The pseudoplastic parameter K in Eq. (3) is set to 0.4 and 1.0 s^{-1} for the 1:2 and 1:4 mixtures, respectively.) The solid and dotted curves corresponds to ω_{disk} of 6.3 and 2.1 rad/s, respectively.

obtained for LB films of the DS-C$_{22}$ 1:1, 1:2, and 1:4 mixtures prepared by using the rotating-disk method are plotted against the inverse of the distance between the center of the disk and the position of the deposition, d^{-1}. In the 1:4 case, P_2 decreases with decreasing d and saturates around $d=5$ cm. ($|P_2|$ increases with decreasing d for $d<8$ cm.) The difference between the data for $\omega_{disk}=6.3$ and 2.1 rad/s is unexpectedly small. The saturated P_2 (≈-0.4) has almost the same absolute value and the opposite sign with the normal dipping (without disk) case. This clearly demonstrates the effect of the rotating disk as it was already reported for other chemical systems [15]. On the contrary, in the 1:1 case P_2 decreases with decreasing d more gradually and the saturation occurs only at small d. The saturation value is also about -0.4 with $\omega_{disk}=6.3$ rad/s. With $\omega_{disk}=2.1$ rad/s the effect of the rotating disk is not apparent for $d>6$ cm. For such a system, higher rotation speed is needed to induce
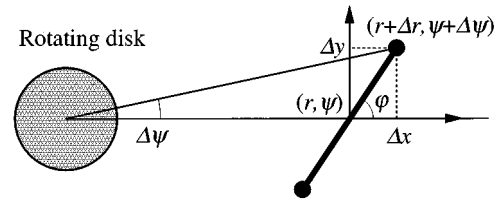

FIG. 11. Geometry in the dumbbell model.

similar effects compared to the 1:4 system. The observed macroscopic inhomogeneity of this monolayer is supposed to be responsible for such behavior. In the 1:2 case P_2 saturates around $d=5$ cm, as in the 1:4 case, but its maximum absolute value is smaller than both the 1:4 and 1:1 cases. This difference can be related to the change in the shearing rate with the distance d and the nature of the monolayer.

C. Dumbbell model

Here, we model the orientation mechanism of the mesoscopic domains in a Langmuir film at the gas-liquid interface in order to interpret the experimental results described above. The so-called ''dumbbell model'' [42], where the mesoscopic domains are treated as dumbbells, is adopted to calculate the orientation distribution function of the domains, as in the case of the ''flow-induced orientation model'' of Sugi and co-workers [11–13]. We define the cylindrical laboratory system (r,ψ) and the Cartesian local system $(\Delta x,\Delta y)$ whose origins are fixed, respectively, at the center of the rotating disk and at the center of the dumbbells (Fig. 11). The rotation speed $\dot{\varphi}$ of a mesoscopic rodlike domain can be calculated as follows. The center of the dumbbells rotates around the center of the rotating disk with the angular velocity of the monolayer $\omega(r)$. We treat the matrix part of the monolayer and domains other than the one under consideration as a continuous medium. We neglect the interaction between this continuous medium and the rod part of the dumbbells. On the other hand, the ball parts are assumed to be fixed in the medium

$$\frac{\partial}{\partial t}\begin{bmatrix}r+\Delta r\\\psi+\Delta\psi\end{bmatrix}=\begin{bmatrix}0\\\omega+(d\omega/dr)\Delta r\end{bmatrix},\qquad(6)$$

where t denotes the time. Considering the time derivative of $\tan\varphi=\Delta y/\Delta x\approx r\Delta\psi/\Delta x$ we obtain

$$\dot{\varphi}\equiv\frac{\partial\varphi}{\partial t}=G\,\cos^2\varphi,\qquad(7)$$

where $G=rd\omega(r)/dr$ is the shearing rate. It should be noted that the dumbbells are in a ''simple shear'' field, which is the sum of ''pure shear'' and pure rotation fields and then $\dot{\varphi}$ has the same sign for all φ ($\dot{\varphi}<0$ when $G<0$). This means there is no mechanically stable point. Note that the dumbbells are in a ''pure stretch'' field in the case of the transfer-induced orientation of Sugi and co-workers [11–13] and in the ''four-roll mill'' case of Friedenberg et al. [16,17], respectively.

The orientation distribution function of the mesoscopic domains at time t, $f(\varphi,t)$, is determined by the compromise
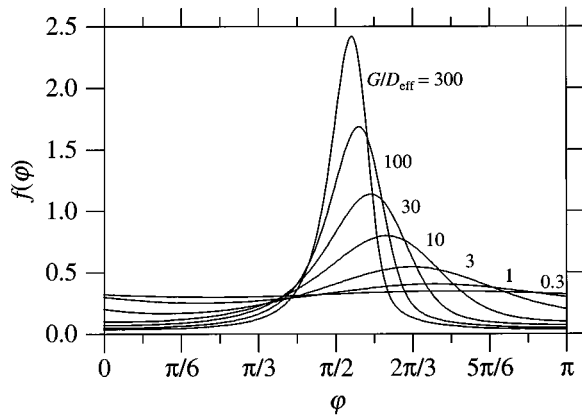
FIG. 12. Examples of the orientation distribution function of mesoscopic rodlike domains in a Langmuir film with a rotating disk calculated by using the dumbbell model.

between the effect of the shearing and the rotatory diffusion. The rotatory diffusion equation for the dumbbells is given by

$$\frac{\partial f(\varphi,t)}{\partial t} = -\frac{\partial}{\partial \varphi}\left(\dot{\varphi} - D_{\text{eff}}\frac{\partial}{\partial \varphi}\right)f(\varphi,t), \qquad (8)$$

where D_{eff} is the effective *rotatory* diffusion constant [11,12]. Friedenberg *et al.* [16] have introduced a nematic potential into the above equation, which may improve the model especially when it is applied to mesogenic materials. However, DS is not a liquid crystal and we use this equation in the present form for simplicity. In the stationary state, the left-hand side of Eq. (8) is zero and we obtain

$$f(\varphi) = A \exp\left(\frac{G\varphi}{2D_{\text{eff}}} + \frac{G\sin\varphi}{4D_{\text{eff}}}\right)$$
$$\times \left[\int_0^\varphi \exp\left(-\frac{G\varphi'}{2D_{\text{eff}}} - \frac{G\sin\varphi'}{4D_{\text{eff}}}\right)d\varphi' + B\right]. \quad (9)$$

Here, A is the normalization factor. The constant B is determined by the cyclic boundary condition of $f(\varphi+\pi) = f(\varphi)$, which is required by the symmetry of the dumbbells [43]. It is noted that for the present DS-C_{22} mixed system, *rotatory* yield value behavior was suggested [12]. In this case we should rewrite G/D_{eff} as

$$\frac{G}{D_{\text{eff}}} = \frac{\zeta G - \tau_0}{k_B T}, \qquad (10)$$

according to Sugi and co-workers. Several examples of $f(\varphi)$ are indicated in Fig. 12 for given G/D_{eff} values. The lack of a mechanically stable point induces the asymmetry in the curves of this figure.

When we neglect the effect of the dipping process and the disturbance of the monolayer flow due to the substrate immersion across the monolayer [19], Eq. (9) is basically applicable also to LB films. In the LB case, however, we normally have different types of monolayers: monolayers deposited during the upward and downward strokes of the substrate, and monolayers deposited onto each side of the substrate. By taking into account the mirror symmetry due to this situation, the orientation distribution function of the do-

mains in LB films is written as $[f(\varphi)+f(\pi-\varphi)]/2$. Since $[f(\varphi)+f(\pi-\varphi)]=[f(-\varphi)+f(\pi+\varphi)]$, Eq. (5) can be used to calculate the total P_2 parameter. The order parameter $P_2^{\text{domain|substrate}}$ is then written by the convolution of f and cosine functions:

$$P_2^{\text{domain|substrate}} = \frac{1}{2}\int_0^\pi \cos 2\varphi [f(\varphi)+f(\pi-\varphi)]d\varphi. \tag{11}$$

D. Comparison of the observed in-plane orientation and the proposed model

The above model for the rotating-disk method may be applicable to the DS-C_{22} 1:4 mixed system, since for this system regular monolayer flow was observed and the absolute P_2 values in the LB films transferred with and without a rotating disk are almost identical. Note that the monolayer flow of this material induced by a rotating disk is given by Eq. (3) with $K=1.0\,\text{s}^{-1}$ and $r_{\text{trough}}=d+d'$, where $d' = 2.4$ cm is the distance between the substrate and the trough edge. We have found that the parameter values of $P_2^{\text{moment|domain}}=0.55$, $\zeta=7\times10^{-12}$ erg s, and $\tau_0=6\times10^{-14}$ erg make the simulation based on Eq. (9) fairly acceptable [Fig. 10(c)]. It should be mentioned that these parameter values also give acceptable P_2 simulations based on the flow orientation model [12] for the LB films fabricated without a rotating disk [44].

The discrepancy between the simulated curves and the experimental data is not negligible in the large d (>8 cm) and small d (<3.5 cm) regions. The discrepancy in the large d region is probably due to the monolayer flow caused by the transfer: the effect of the shearing (introduced by the disk) and that of the stretching (introduced by the transfer) are comparable. This may also cause the relatively low reproducibility of the P_2 data in this region. The origin of the discrepancy in the small d region is not clear at present, but we speculate that the substrate itself disturbs the monolayer flow and reduces the absolute P_2 value. The difference between the simulated curves for $\omega_{\text{disk}}=6.3$ and 2.1 rad/s is small, corresponding to a tiny difference in the P_2 data. The nonlinearity of the monolayer flow and the saturation behavior of the P_2 value are the causes of this small difference. This result suggests that too large ω_{disk} is useless in the rotating-disk method, if the given monolayer exhibits a regular flow.

The cause of the observed smaller efficiency of the rotating-disk method in the 1:2 mixture case is surely related to the effect of mixing on the viscolelastic behavior of the monolayer and may be related to the dipping process, but remains unclear at present. For the 1:1 mixture we have a fairly large absolute P_2 value with the rotating-disk method especially in case of small d, i.e., small r_{trough}, although the observed flow in the monolayer was not regular with large r_{trough}.

Finally, we would like to point out that the present study provides a guideline for designing a rotating-disk apparatus. The rotation speed of the disk is *not* neccessarily large (2 rad/s is sufficient), but a larger disk may be useful for the following reason. The magnitudes of side effects such as surface waves may be proportional to r_{disk}, $r_{\text{disk}}\omega_{\text{disk}}$, or

$r_{disk}^2 \omega_{disk}$ [45]. With the same $r_{disk}^2 \omega_{disk}$, we can produce larger $\omega(r_{disk} + d'')$ by increasing r_{disk}, when the distance between the substrate and the edge of the disk, d'', is fixed, because $\omega(r)$ decreases more rapidly than r^{-2} as discussed in Sec. IV. Another important point is that small r_{trough} may have an advantage: when r_{trough} is smaller than the size of the macroscopic structure, the monolayer flow could be regular, even though the monolayer has macroscopic inhomogenity as in the 1:1 mixture case. In other words, with small r_{trough} the required homogeneous area is reduced. Furthermore, smaller trough enhances $|d\omega/dr|$ and then enhances G.

VI. CONCLUSION

We have demonstrated that the rotating-disk method is effective also for the Langmuir and Langmuir-Blodgett films of the DS-C$_{22}$ mixed system, after performing a general characterization of these films. However, the efficiency depends on the mixing ratio, which changes the macroscopic homogeneity and the viscoelastic properties of the monolayer. We observed monolayer flow induced by a rotating disk and showed characteristic nonlinearity and rapid decrease of the angular velocity with the distance to the disk, implying the important role of the pseudoplasticity of the monolayers. Based on this *in situ* observation of the flow, we proposed an analytical model for the rotating-disk method. Although the real system is more complicated, the proposed model is valuable to estimate the in-plane order of the film, when the monolayer flow is regular and not seriously disturbed by the deposition process. Moreover, they have figured out the important factors in the rotating-disk method. When the effect of the flow introduced respectively by the disk and by the monolayer transfer are comparable, the situation is much more complicated and the present analytical model should be modified in order to take into account both effects. In-plane orientation under such conditions is qualitatively discussed elsewhere [19]. Overall, such experiments demonstrate the possibility of characterizing and understanding the hydrodynamical process in a Langmuir film in order to obtain a better control of the in-plane orientation at the interface and also in LB films to build up new films having in-plane anisotropic properties. Along this line, development of an improved version of the rotating-disk method is now in progress [46].

ACKNOWLEDGMENTS

APPENDIX

1. Velocity field with a dissipative interaction

A rigorous theory for the infinite system is known [36]. However, we treat this problem phenomelogically, because generally the dimensions of the trough are not large enough to assume that they are infinite. In the first-order approximation, we assume that this dissipative force applied to the ring

$[r, r+dr]$ is proportional to the product of the flow velocity, $r\omega$, and the area of the ring, $2\pi r\,dr$, according to the usual manner. The proportional coefficient is defined as $-\eta_{diss}$. (In other words, ''friction'' between the monolayer and the bottom of the trough mediated by the water subphase is taken into the account.) This phenomenological term is added to the torque, $M(r) - M(r+dr)$:

$$\frac{d}{dr}[2\pi r^2 \sigma]dr + r[-2\pi r^2 \omega]dr = 0. \qquad (A1)$$

This second-order differential equation can be transformed to a degenerated hypergeometric type, whose solution is written by using the first-order modified Bessel functions, I_1 and K_1, as

$$\omega = C_2 r^{-1} I_1\left(\sqrt{\eta_{diss}/\eta_L}\,r\right) + C_3 r^{-1} K_1\left(\sqrt{\eta_{diss}/\eta_L}\,r\right), \qquad (A2)$$

where C_2 and C_3 should be determined by the boundary conditions. Unfortunately Eq. (A2) is linear with respect to ω_{disk} and does not fit the obtained data (especially the large r region) for any given ω_{disk}.

2. Velocity field with non-Newtonian viscosity represented by the lowest order correction terms

a. Bingham yield value case

The Bingham yield-value behavior of the monolayer can be expressed as

$$\sigma = \eta_1 G + \eta_0. \qquad (A3)$$

Here, η_1 is the Newtonian viscosity and η_0 is the yield value whose sign is identical with that of G. Then we readily obtain the next solution instead of Eq. (1):

$$\omega = \frac{M}{4\pi\eta_1} r^{-2} + C_1 - \frac{\eta_0}{\eta_1}\ln r. \qquad (A4)$$

The rotation velocity expressed by Eq. (A4) decreases more rapidly with increasing r than the Newtonian case. However, the tendency of the nonlinearity introduced by the yield value (ω decreases more rapidly for *smaller* ω_{disk}) is opposite to the observed one and Eq. (A4) does not fit the obtained data (especially the large r region) for any given ω_{disk}.

b. Dilatant case

In the lowest-order approximation the dilatant behavior can be expressed as

$$\sigma = \eta_1 G + \eta_3 G^3, \qquad (A5)$$

where η_3 (>0) denotes the degree of the nonlinearity. From the torque equation and (A5) we obtain

$$\left(\frac{d\omega}{dr}\right)^3 + \frac{\eta_1}{\eta_3} r^{-2}\frac{d\omega}{dr} + \frac{M}{2\pi\eta_3} r^{-5} = 0. \qquad (A6)$$

The only real solution of this equation is given by the next equation:

$$\omega = \omega_{\text{disk}} + \int_{r_{\text{disk}}}^{r} \left\{ \left[\left(\frac{M\rho^{-5}}{4\pi\eta_3} \right)^2 + \frac{\eta_1^3}{\eta_3^3} \frac{\rho^{-6}}{27} \right]^{1/2} - \frac{M\rho^{-5}}{4\pi\eta_3} \right\}^{1/3} d\rho$$

$$- \int_{r_{\text{disk}}}^{r} \left\{ \left[\left(\frac{M\rho^{-5}}{4\pi\eta_3} \right)^2 + \frac{\eta_1^3}{\eta_3^3} \frac{\rho^{-6}}{27} \right]^{1/2} + \frac{M\rho^{-5}}{4\pi\eta_3} \right\}^{1/3} d\rho,$$

(A7)

where M should be determined by the boundary condition of $\omega(r_{\text{trough}}) = 0$. The angular velocity expressed by this equation decreases more gradually with increasing r than the Newtonian case. In addition, the tendency of the introduced nonlinearity is opposite to the observed one.

c. Pseudoplastic case

In the lowest-order approximation the pseudoplastic behavior can be expressed also by Eq. (A5), but with negative η_3. The physical solution of $d\omega/dr$ in Eq. (A6) should be zero or negative (real). This requires the condition of

$$M^2 < \frac{8\pi}{27} \frac{(\eta_1)^3}{(-\eta_3)} r^4,$$

(A8)

showing that the higher-order corrections are required in Eq. (A5) in the case of larger torque. Assuming the condition (A8) we obtain

$$\omega = \omega_{\text{disk}} + \int_{r_{\text{disk}}}^{r} \left(\frac{2\eta_1}{3\eta_3} \rho^{-2} \right)^{1/2}$$

$$\times \cos\left\{ \frac{2\pi}{3} \right.$$

$$\left. - \frac{1}{3} \tan^{-1} \frac{[(2\eta_1\rho^{-2}/3\eta_3)^3 - (M\rho^{-5}/2\pi\eta_3)^2]^{1/2}}{M\rho^{-5}/2\pi\eta_3} \right\} d\rho.$$

(A9)

This solution suggests that the pseudoplastic property of the monolayer could cause the rapid decrease in $\omega(r)$ and introduce a nonlinearity to the system in the right way. Unfortunately, however, this solution is very close to the Newtonian one written by Eq. (1), implying that the torque given by the experimental conditions is large enough to break down the lowest-order approximation. We have therefore selected Eyring's formulation [see Eq. (2) in the main text] to describe this pseudoplastic case.

---

[1] See, for example, A. Ulman, *An Introduction to Ultrathin Organic Films* (Academic Press, New York, 1991).

[2] A. Ferencz, R. Ries, and G. Wegner, Angew. Chem. Int. Ed. Engl. **32**, 1184 (1993).

[3] T. Fukui, M. Saito, M. Sugi, and S. Iizima, Thin Solid Films **109**, 247 (1983).

[4] S. Kuroda, K. Ikegami, M. Sugi, and S. Iizima, Solid State Commun. **58**, 493 (1986).

[5] H. Nakahara and D. Möbius, J. Colloid Interface Sci. **114**, 363 (1986).

[6] T. Sauer, T. Arndt, D. Batchelder, A. A. Kalachev, and G. Wegner, Thin Solid Films **187**, 357 (1990).

[7] K. Ikegami, S. Kuroda, Y. Tabe, K. Saito, M. Sugi, M. Matsumoto, T. Nakamura, and Y. Kawabata, Jpn. J. Appl. Phys. 1 **31**, 1206 (1992).

[8] M. Vandevyver, P.-A. Albouy, C. Mingotaud, J. Perez, A. Barraud, O. Karthaus, and H. Ringsdorf, Langmuir **9**, 1561 (1993).

[9] S. Pfeiffer, C. Mingotaud, C. Garrigou-Lagrange, P. Delhaés, A. Sastre, and T. Torres, Langmuir **11**, 2705 (1995).

[10] C. Jego, N. Leroux, B. Agricole, M. Mauzac, and C. Mingotaud, Liq. Cryst. **20**, 691 (1996).

[11] N. Minari, K. Ikegami, S. Kuroda, K. Saito, M. Saito, and M. Sugi, Solid State Commun. **65**, 1259 (1988).

[12] N. Minari, K. Ikegami, S. Kuroda, K. Saito, M. Saito, and M. Sugi, J. Phys. Soc. Jpn. **58**, 222 (1989).

[13] Y. Tabe, K. Ikegami, and M. Sugi, J. Appl. Phys. **73**, 905 (1993).

[14] It has been reported that the compression of the monolayer can also induce the in-plane organization, but this ''compression orientation'' does not seem to be efficient enough to obtain large in-plane anisotropy (See, Ref. [7]).

[15] C. Mingotaud, B. Agricole, and C. Jego, J. Phys. Chem. **99**, 17 068 (1995).

[16] M. C. Friedenberg, G. G. Fuller, C. W. Frank, and C. R. Robertson, Macromolecules **29**, 705 (1996).

[17] M. C. Friedenberg, G. G. Fuller, C. W. Frank, and C. R. Robertson, Langmuir **12**, 1594 (1996).

[18] In this paper we neglect the effect of the dipping process in the rotating-disk method for simplicity, because the used sharing rate is relatively high. Discussion about this point will appear in Ref. [19].

[19] K. Ikegami, C. Mingotaud, and P. Delhaes, Supramol. Sci. (to be published).

[20] The software was obtained from ''http://rsb.info.nih.gov/nih-image/''.

[21] J. Breton, M. Michel-Villaz, G. Paillotin, and M. Vandevyer, Thin Solid Films **13**, 351 (1972).

[22] P.-A. Chollet and J. Messier, Thin Solid Films **99**, 197 (1983).

[23] K. Iriyama, F. Mizutani, and M. Yoshimura, Chem. Lett. **1980**, 1399 (1980).

[24] K. Iriyama, M. Yoshimura, and Y. Ozaki, Thin Solid Films **132**, 229 (1985).

[25] Y. Fujimoto, Y. Ozaki, M. Takayanagi, M. Nakata, and K. Iriyama, J. Chem. Soc. Faraday Trans. **92**, 413 (1996).

[26] Y. Fujimoto, Y. Ozaki, and K. Iriyama, J. Chem. Soc. Faraday Trans. **92**, 419 (1996).

[27] Y. Ozaki, K. Iriyama, T. Iwasaki, and H. Hamaguchi, Appl. Surf. Sci. **33/34**, 1317 (1988).

[28] M. Yoneyama, T. Nagao, and T. urayama, Chem. Lett. **1989**, 397 (1989).

[29] A. Miyata, D. Heard, Y. Unuma, and Y. Higashigaki, Bull. Chem. Soc. Jpn. **66**, 999 (1993).

[30] G. L. Gaines, *Insoluble Monolayers at Liquid-gas Interfaces* (John Wiley, New York, 1966).

[31] D. Möbius, Adv. Mater. **7**, 437 (1995).

[32] The observed area of vortices increases as decreasing π or decreasing ω_{disk}. A concentric LB trough may be needed to

precisely determine the viscoelastic properties of the monolayers. However, our purpose is to know the velocity field of the monolayers, which cause the in-plane orientation of the mesoscopic domains, rather than to perform a rheological study.

[33] G. K. Batchelor, *An Introduction to Fluid Dynamics* (Tokyo Denki University Press, Tokyo, 1972).

[34] P. C. Hiemenz, *Principles of Colloid and Surface Chemistry*, 2nd ed. (Marcel Dekker, New York, 1986), p. 173.

[35] This value is identical with the distance between the center of the disk and one of the walls of the trough really used.

[36] G. C. Goodrich and A. K. Chatterjee, J. Colloid Interface Sci. **34**, 36 (1970).

[37] H. Eyring, J. Chem. Phys. **4**, 283 (1936).

[38] H. Eyring, *The Theory of Rate Processes*, edited by S. Glasstone, K. J. Laidler, and H. Eyring (McGraw-Hill, New York, 1941), Chapt. IX, pp. 480–483.

[39] In Refs. [37] and [38] Eyring used microscopic parameters instead of the phenomenological parameters η and K in Eq. (2), but in this paper we do not intend to discuss the origin of the pseudo-plasticity and these phenomenological parameters are convenient for our purpose. We write the proportinal coefficient as ηK simply to give η the dimension of viscosity.

[40] R. Miller, R. Wüstneck, J. Krägel, and G. Kretzschmar, Colloids Surf. **111**, 75 (1996).

[41] η_L cannot be obtained without measuring the torque.

[42] N. Saito, *Introduction to Polymer Physics* (Syokabo, Tokyo, 1967).

[43] $B = \{1/[\exp(-\pi G/2D_{\mathrm{eff}})-1]\}\int_0^\pi \exp(-G\varphi'/2D_{\mathrm{eff}} - G\sin2\varphi'/4D_{\mathrm{eff}})d\varphi'$.

[44] In Ref. [12] Sugi *et al.* obtained $P_2^{\mathrm{moment|domain}}=0.4$, $\zeta=5\times10^{-13}$ erg s and $\tau_0=6\times10^{-14}$ erg.

[45] When the rotation axis of the disk tilts, the difference in the height at the disk edge is proportional to r_{disk}. The velocity at the disk edge is $r_{\mathrm{disk}}\omega_{\mathrm{disk}}$. The magnitudes of side effects may be proportional to the former, the latter or the product of the both values.

[46] K. Ikegami, C. Jego, C. Mingotaud, and P. Delhaés, Jpn. J. Appl. Phys. 2 **36**, L883 (1997).